# 151: Hydraulics of Wells and Well Testing

**PHILIPPE RENARD**

*University of Neuchâtel, Neuchâtel, Switzerland*

*Well testing and well hydraulics play a major role in applied hydrogeology. While well hydraulics aims at modeling the groundwater behavior in response to a perturbation – such as pumping – in a well, well testing aims at using these models in an inverse approach to infer the properties of the aquifer or of the well itself. The history of well hydraulics and well testing started in 1863 with Dupuit, who developed the first analytical solution to model radial flow to a well in steady state. In 1935, Theis published the most important analytical solution. The Theis solution assumes that the aquifer is confined, bidimensional, homogeneous, and isotropic. Subsequently, numerous models have been developed with the aim to enlarge the domain of applications. This article presents a brief review of these various models and describes their behavior in terms of drawdown and log derivative of the drawdown. The log derivative is used as a tool to help in the identification of the most appropriate model when analyzing field data.*

## INTRODUCTION

Well hydraulics is the part of groundwater hydraulics (*see* **Chapter 149, Hydrodynamics of Groundwater, Volume 4**) that deals specifically with aquifer response to hydraulic perturbations in a well. Well tests are field tests in which the hydraulic response is measured and analyzed. Well hydraulics and well testing are intimately related since they respectively solve the direct and the inverse problem. As any inverse problem (*see* **Chapter 156, Inverse Methods for Parameter Estimations, Volume 4**), the well-test interpretation suffers from nonuniqueness. Usually this is solved by assuming a very simple model with a very small number of parameters as compared to the number of field observations. The problem is then over-determined and has a unique solution when a model has been chosen. The difficulty is to identify the model that best represents reality. Often, different models will show the same type of response and they will not be distinguishable (e.g. unconfined aquifer and double porosity aquifer). In addition, the measurements may not be sufficient to see all the typical phases of a given model, either because the very early phase is too rapid and is not recorded or conversely the late phase is not recorded because the test does not last long enough. This long introductory remark highlights the fact that despite the relatively large number of models that are available, the practitioner will always be confronted with the dilemma of a nonunique interpretation.

Since groundwater is mainly extracted by wells and well testing represents the main field method for determining the hydraulic properties of the subsurface, much research has been conducted in this area. We can trace the first publication on well hydraulics to Dupuit (1863), who proposed the first series of analytical solutions to steady-state flow to a well in idealized confined or unconfined aquifers. Since then, there has been a continuous and parallel development of analytical models and well-testing procedures. This is reflected by the numerous books published, both in the fields of hydrogeology (Batu, 1998; Butler, 1998; Dawson and Istok, 1991; Hantush, 1964; Kruseman and Ridder, 1992; Lebbe, 1999; Lee, 1999; Walton, 1996) and petroleum engineering (Bourdet, 2002; Earlougher, 1977; Horne, 1995; Raghavan, 1993; Streltsova, 1988).

The aim of this article is to provide an introduction to this field. The article is not intended to be used as a manual or to be exhaustive. Rather, it includes some of the most important historical findings with sufficient details to permit the reader to apply the techniques and understand the basic concepts and equations. Additional aspects are covered in a cursory manner, simply to direct the reader to pertinent sources of information. Some aspects have arbitrarily been

Encyclopedia of Hydrological Sciences. Edited by M G Anderson.

left aside such as anisotropy, pulse tests, sinusoidal tests, horizontal wells, and so on.

The article is organized in five sections. The first section presents an overview of well-testing procedures and interpretation methodologies. The second introduces the basic equations of groundwater flow to a well in an ideal confined aquifer as well as the steady-state solution for such a case. The third considers the Theis solution for the transient regime in the ideal confined aquifer. The fourth reviews different nonidealities that can affect the response of an aquifer to pumping in a well. The last briefly considers some other types of hydraulic perturbations.

## WELL TESTING

Well tests are conducted with two major objectives. One is to determine the properties of geological formations for a broad range of applications from groundwater exploration to waste-disposal-site evaluation. The other objective is to evaluate the hydraulic properties of the production well itself in order to design the exploitation scheme (depth of the pump, pumping rate) or to evaluate the well efficiency.

The fundamental principle of well testing is the imposition of a hydraulic perturbation in the well and monitoring the aquifer response. Testing procedure may be classified according to the type of perturbation, and to the type and location of response monitoring. Note that the typology is not mutually exclusive.

- *Single well test*: The perturbation and the monitoring are conducted in the same borehole.
- *Interference test*: The perturbation and the monitoring are conducted in separate boreholes.
- *Pumping test*: The aquifer is perturbed by pumping. It can either be a single well test or an interference test. Generally the pumping rate is constant, but variable-pumping-rate tests can also be interpreted. An *injection test* is similar to a pumping test, but water is injected rather than being extracted.
- *Step-drawdown test*: A single well test with a series of successive constant pumping rates.
- *Buildup or recovery test*: It follows a pumping test. After the pump has been stopped, the recovery to the initial level is observed, either in the pumping well or in observation wells.
- *Constant head test*: The head is maintained constant and the water discharge is recorded in the perturbation well. Head changes can be recorded in observation boreholes.
- *Slug test*: The perturbation is a sudden modification of the head in the well, the response is the head variation in the well itself or in observation boreholes.
- *Packer test*: It can be any of the above tests, but it is conducted in an interval of the well isolated with the help of packers. The packers are inflatable or mechanical and allow testing a distinct zone within a well.

Once data – time series of pressures or heads and/or discharge rates – have been recorded from one of the above tests, the interpretation procedure follows fours steps.

- *Data preprocessing*. The data are converted into adequate units, outliers and trends are removed.
- *Model identification*. A conceptual and mathematical model is chosen based on the geological information available and based on a qualitative analysis of the data.
- *Parameter identification*. The physical parameters of the model are obtained by fitting the theoretical response to the observed response. This is a typical inverse problem (*see* **Chapter 156, Inverse Methods for Parameter Estimations, Volume 4**).
- *Quality control*. The adequacy of the model must be checked. A statistical analysis of the discrepancies between the model and the data is conducted in order to test the validity of the interpretation.

While standard well-test analysis used to be based on manual type curve matching or straight-line analysis, the methodology is now mostly computerized for all the four above introduced steps. As a consequence, new methods have been intensively developed in the last twenty years. The benefits of interactive graphics and data handling with computers are obvious. Computerized analysis has allowed handling large data sets directly recorded in the field with electronic pressure gauges and data acquisition systems. Moreover, it has allowed the introduction of the systematic use of the logarithmic derivative of the drawdown as a tool for model identification (Bourdet *et al.*, 1989). Numerical Laplace inversion has broaden the range of models that would be tedious to program otherwise (Dougherty, 1989; Moench and Ogata, 1984). Numerical convolution has allowed interpretation of continuously variable pumping rate test. Automatic model fitting with different optimization algorithms became also possible (McElwee, 1980; Rosa and Horne, 1991), opening the way to a more objective model fitting as well as to a statistical analysis of the results. Finally, computerized data analysis has also allowed the application of general purpose or specifically developed numerical models (*see* **Chapter 155, Numerical Models of Groundwater Flow and Transport, Volume 4**) to interpret field data (Lavenue and de Marsily, 2001; Lebbe, 1999; Pinder and Bredehoeft, 1968), or to forecast the impact of wells on aquifers.

With the expansion of personal computing technology, a large number of well test analysis software has been developed both in the groundwater and petroleum engineering fields. Some of them are freely available through various institutional or academic internet sites (**`http://water.usgs.gov/nrp/gwsoftware/`**,

**http://water.usgs.gov/software/**, **http://www.kgs.ukans.edu/Datasale/suprpump.html**, **http://home.olemiss.edu/~acheng/software/index.html**) or under commercial licenses **http://www.scisoftware.com/products/cat_pump_test/cat_pump_test.html**. Amongst other commercial software, and based on the author's experience, one of the best available software package from the petroleum engineering field is Saphir (**http://www.kappaeng.com/Saphir/index.asp**).

## THE IDEAL CONFINED AQUIFER

### Groundwater-Flow Equation Around a Well

Following Dupuit (1863), we consider an idealized aquifer (Figure 1a). The aquifer is assumed to be infinite in lateral extent, fully confined (no recharge or leakage), two dimensional (large extension compared to its thickness), having a homogeneous transmissivity and storativity. At time zero, pumping starts at a constant rate in the well. If we assume that the heads are constant in space prior to pumping, the flow field will be radial (Figure 1b). All flow lines will converge toward the well as straight lines. If we consider a cylinder of radius $r$ centered on the well, the total water flux $Q(r)$ [$L^3T^{-1}$] flowing through the cylinder is given by multiplying the area of the cylinder by the specific discharge calculated according to Darcy's law. This yields the following:

$$Q(r) = -2\pi r T \frac{\partial h}{\partial r} \tag{1}$$

where $T$ [$L^2T^{-1}$] is the transmissivity of the aquifer (hydraulic conductivity multiplied by the aquifer thickness). Since the aquifer is fully confined, and since the water is only slightly compressible, the mass conservation of water between two cylinders during a time interval can be expressed as

$$\frac{\partial Q}{\partial r} = -2\pi r S \frac{\partial h}{\partial t} \tag{2}$$

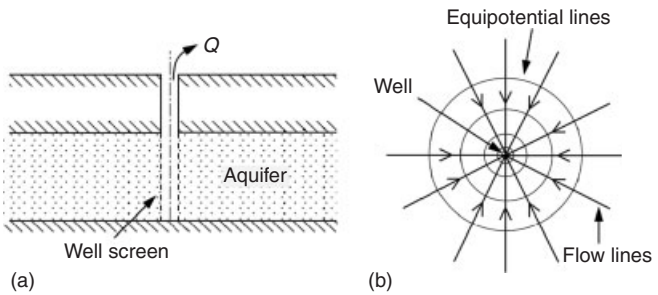


**Figure 1** Schematic illustration of an idealized confined aquifer (a) and radial converging flow (b) to a fully penetrating pumping well in such aquifer

with $S$[−] representing the storage coefficient and $t$ the time. Combining equations (1) and (2) yields

$$\frac{1}{r}\frac{\partial h}{\partial r} + \frac{\partial^2 h}{\partial r^2} = \frac{S}{T}\frac{\partial h}{\partial t} \tag{3}$$

Equation (3) is linear, and has been derived by assuming for didactic reasons that the heads were constant prior to pumping. But this is not a necessity. In general, equation (3) will be written instead in terms of drawdown $s$ [L], defined as the difference between the head $h_0$ as it would have been without pumping minus the actual head $h$ in the aquifer during pumping (Figure 2).

$$s(t) = h_0(t) - h(t) \tag{4}$$

While $h$ is the solution to equation (3) with complex boundary and initial conditions, $s$ is another solution with much simpler initial and boundary conditions.

It is important to note that when an aquifer is unconfined, the previous equations are not rigorously valid. They can only be applied if the saturated thickness is large compared to the drawdown. Other equations, which are nonlinear, were derived by Dupuit, under additional simplifying assumptions but are of limited applicability. In the following, we restrict ourselves to the case of confined aquifers unless we specify otherwise.

### The Dupuit–Thiem Solution in Steady State

Once again, following Dupuit (1863), we consider the case in which flow to a well is in dynamic equilibrium, that is, steady state. The pumping rate $Q$ is constant and the head in the aquifer varies in space but not in time. Under this assumption, the flow $Q(r)$ through any cylinder must be identical to the pumping rate $Q$. Hence, we can directly integrate equation (1), and making use of the definition of the drawdown to find

$$s(r) = -\frac{Q}{2\pi T}\ln(r) + A \tag{5}$$

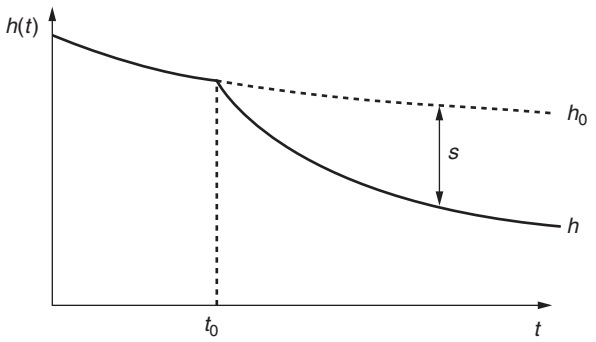


**Figure 2** Definition of the drawdown

$A$ is a constant of integration. To eliminate $A$, Dupuit defines rather arbitrarily a radius $R$ at which the head $h_0$ is not affected by the pumping. A better technique was proposed by Thiem (1906) who considered the drawdown difference $s_1 - s_2$ between two observations points located at distance $r_1$ and $r_2$ from the pumping well. This yields

$$T = \frac{Q}{2\pi(s_2 - s_1)} \ln\left(\frac{r_1}{r_2}\right) \tag{6}$$

Equation (6), known as the *Thiem's formula*, allows determination of the transmissivity T of an aquifer from a constant pumping rate field experiment. Thus, one only has to measure the drawdown difference between two piezometers, and make sure that the difference remains constant and to calculate $T$ with equation (6). Despite that this equation has been derived under steady state assumptions, we will show in Section Relation between Jacob and Thiem solutions that it is also valid for transient conditions for homogeneous aquifers. However, in practice, it should be applied with great care, as the calculated transmissivity is strongly affected by heterogeneities as we will discuss in Section Heterogeneous aquifers.

## THE THEIS SOLUTION

The Theis (1935) solution considers the same geometry as the Dupuit–Thiem solution, but under transient-flow regime. It is the most important analytical solution for well hydraulics because most other transient models tend towards it either for early or late times. Therefore, it can often be used even if the underlying assumptions are not fully satisfied.

### Assumptions and Solution

The Theis model assumes that the aquifer is confined, infinite, homogeneous, and isotropic; the well is fully penetrating the aquifer, the well has a negligible radius and is 100% efficient; the pumping rate $Q$ is constant. The initial condition is set to zero drawdown everywhere within the aquifer prior to pumping.

$$s(r, t = 0) = 0 \tag{7}$$

The boundary conditions consist of zero drawdown at infinity and a fixed flux equal to the pumping rate at the well.

$$\lim_{r\to\infty} s = 0 \tag{8}$$

$$\lim_{r\to 0} 2\pi T r \frac{\partial s}{\partial r} = -Q \tag{9}$$

The solution of equation (3) subject to initial and boundary conditions (7–9) yields the Theis solution

$$s = \frac{Q}{4\pi T} E_1\left(\frac{r^2 S}{4tT}\right) \tag{10}$$

$E_1$ is the exponential integral function. Written in dimensionless form the Theis solution is

$$s_D = \frac{1}{2} E_1\left(\frac{r_D^2}{4t_D}\right) \tag{11}$$

where $s_D$, $r_D$, and $t_D$ represent respectively the dimensionless drawdown, dimensionless radius, and dimensionless time defined as

$$s_D = \frac{2\pi T}{Q} s, \quad r_D = \frac{r}{r_W}, \quad t_D = \frac{Tt}{r_W^2 S} \tag{12}$$

with $r_W$ being the radius of the well. Note that the logarithmic derivative of the drawdown is as follows (Chow, 1952):

$$\frac{\partial s_D}{\partial \ln(t_D)} = t_D \frac{\partial s_D}{\partial t_D} = \frac{1}{2} \exp\left(-\frac{r_D^2}{4t_D}\right) \tag{13}$$

Equation (11) describes how the drawdown evolves in time and space as a function of transmissivity and storativity of the aquifer and as a function of the pumping rate. Since Bourdet *et al.* (1983), equation (11) together with its logarithmic derivative, equation (13), are usually plotted in log–log scale as a function of $t_D/r_D^2$. It shows that the drawdown increases with time and decreases with radial distance (see Figure 3a). The derivative tends toward a constant value of 0.5 for late time. The spatio-temporal behavior of the cone of depression shows that the shape of the cone is created very quickly, and then the cone moves downward.

### Compression Zone and Radius of Investigation

An important question in well hydraulics and well testing is the definition of the volume of aquifer that is affected by pumping and influences the drawdown behavior. For that purpose, it is useful to calculate the flux of groundwater through a cylinder centered on the well, having a radius $r_D$. This flux, normalized by the pumping rate, is

$$q_D = \frac{q(r_D)}{Q} = \exp\left(-\frac{r_D^2}{4t_D}\right) \tag{14}$$

Figure 4 shows the behavior of equation (14), three zones are distinguishable and evolve with time. At small radial distances, the normalized flux is close to 1. This indicates that the flux is equal to the pumping rate; the aquifer simply transfers water to the well. At infinity, the flux is close to

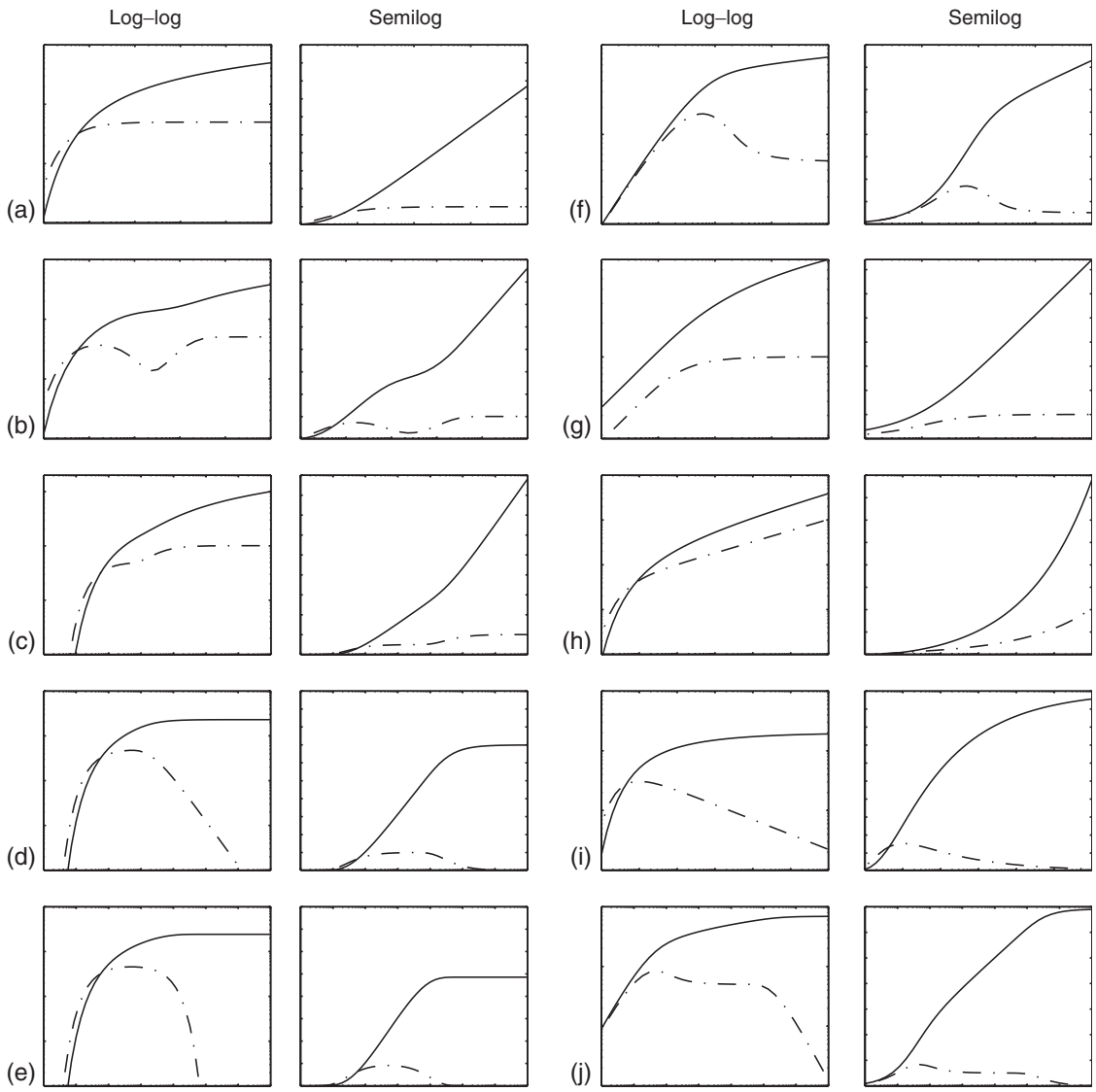


**Figure 3** A synthesis of some typical drawdown behaviors in response to constant pumping rate. The drawdown (solid line) and the log derivative (dashed line) are plotted as a function of time in double-logarithmic or semilogarithmic scale. (a) Theis model: confined ideal aquifer. (b) Unconfined, or double porosity aquifer. c) Confined aquifer with a no-flow boundary. (d) Confined aquifer with a constant head boundary. (e) Leaky aquifer: Hantush and Jacob (1955) model. (f) Single well test with well-bore storage and possibly skin effects. (g) Single vertical fracture having an infinite conductivity. (h) General Radial-Flow model with $n < 2$. (i) General Radial-Flow model with $n > 2$. (j) Single well test with well-bore storage, infinite acting radial flow and constant head boundary (Reproduced from Gringarten *et al.* (1974), by permission of American Geophysical Union)

zero. There, the aquifer is not yet active. At intermediate distances, the fluxes vary from 0 to 1; water is mobilized from the compaction of aquifer and elastic expansion of the water itself. This is the so called *compression zone*, which propagates with time.

The radius of investigation of a pumping test is a concept introduced by Dupuit. It was defined as the radius beyond which the drawdown is zero. For the Theis solution, which never predicts drawdown to be strictly zero, there are several possible and arbitrary definitions depending on what is considered as being a negligible drawdown. An elegant possibility is to define the radius of investigation as the radius such that the rate of increase in drawdown with time is maximal (Van Poolen, 1964). Using this definition and calculating the distance at which the second temporal derivative of the drawdown is zero, one finds the simple result:

$$r_{\mathrm{D}}^{i} = 2\sqrt{t_{\mathrm{D}}} \quad \text{or} \quad r^{i} = 2\sqrt{\frac{Tt}{S}} \tag{15}$$

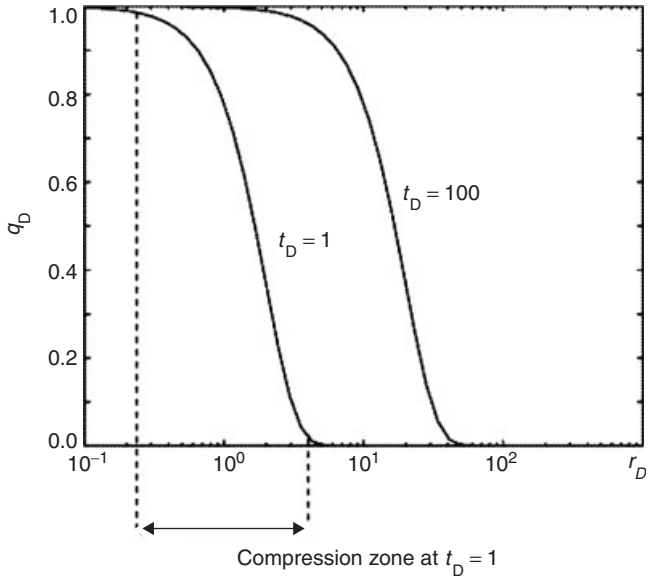


**Figure 4** Normalized groundwater flux as a function of radial distance from the well and time

Most alternative definitions of the radius of investigation yield similar equations, being functions of the square root of dimensionless time, but with scaling factors varying from 1.5 to 4.3. All these definitions illustrate the arbitrariness of the concept, but interestingly they all locate the radius of investigation within the compression zone.

More recently, the question of the extension of the investigation domain during a pumping test has been formulated in the framework of spatial filtering functions and heterogeneous transmissivity fields (Beckie, 2001; Oliver, 1993). These authors found that the investigation area is more or less an ellipse that encloses the pumping and the observation wells, but the influence of the heterogeneities within this ellipse is not spatially uniform.

## Approximation of the Exponential Integral Function

Applying equations (10) or (11) for well-test interpretation or to design exploitation schemes requires the use of the exponential integral function. It is generally directly available in most mathematical software but, if necessary, it can be calculated with a polynomial and rationale approximations (Abramowitz and Stegun, 1970). For small $x$, the approximation is

$$\begin{aligned} &0 \le x \le 1 \\ &E_1(x) = -\gamma - \ln(x) + a_1 x + a_2 x^2 \\ &\qquad + a_3 x^3 + a_4 x^4 + a_5 x^5 + \varepsilon \\ &|\varepsilon| < 210^{-7} \end{aligned} \tag{16}$$

with $\gamma$ being the Euler constant and

$$\begin{aligned} \gamma &= 0.57721566 \quad a_2 = -0.24991055 \quad a_4 = -0.00976004 \\ a_1 &= 0.99999193 \quad a_3 = 0.05519968 \quad a_5 = 0.00107857 \end{aligned} \tag{17}$$

For large $x$, the approximation is

$$\begin{aligned} &1 \le x \le \infty \\ &E_1(x) = \frac{1}{xe^x}\left(\frac{x^4 + a_1 x^3 + a_2 x^2 + a_3 x + a_4}{x^4 + b_1 x^3 + b_2 x^2 + b_3 x + b_4}\right) + \varepsilon \\ &|\varepsilon| < 210^{-8} \end{aligned} \tag{18}$$

with

$$\begin{aligned} a_1 &= 8.5733287401 \quad a_2 = 18.0590169730 \\ a_3 &= 8.6347608925 \quad a_4 = 0.2677737343 \\ b_1 &= 9.5733223454 \quad b_2 = 25.6329561486 \\ b_3 &= 21.0996530827 \quad b_4 = 3.9584969228 \end{aligned} \tag{19}$$

## Asymptotic Behavior: the Jacob Solution

Equation (16) shows that the exponential integral $E_1(x)$ tends toward $-\gamma - \ln(x)$ when $x$ tends toward 0. In practice, when the dimensionless number $t_D/r_D^2$ is greater than 10, the Theis solution can be approximated by a simple logarithmic function. This is the so-called Jacob's approximation of the Theis solution (Cooper and Jacob, 1946).

$$s_D \approx \frac{1}{2}\left[\ln\left(\frac{4t_D}{r_D^2}\right) - \gamma\right] \quad \text{or} \quad s \approx \frac{2.30Q}{4\pi T}\log\left(\frac{2.25tT}{r^2 S}\right) \tag{20}$$

Note that when equation (20) is valid, the logarithmic derivative of the drawdown becomes constant.

$$\frac{\partial s_D}{\partial \ln(t_D)} = t_D \frac{\partial s_D}{\partial t_D} = \frac{1}{2} \quad \text{or} \quad \frac{\partial s}{\partial \ln(t)} = \frac{Q}{4\pi T} \tag{21}$$

This relation is used to analyze data sets. One calculates the logarithmic derivative of the measured drawdown and plots it as function of time. When the derivative becomes constant, it indicates that the drawdown has reached a logarithmic asymptote. In petroleum engineering literature, the interval of the data set that shows a constant derivative is identified as the *Infinite Acting Radial Flow* (IARF). During this period of time, one can use safely the logarithmic approximation (18) to interpret the data. If the derivative does not remain constant, the logarithmic approximation cannot be used.

## Relation Between Jacob and Thiem Solutions

When Jacob's approximation is valid in two observation boreholes located at distances $r_1$ and $r_2$ from the pumping well, we can use equation (20) to calculate the drawdown

difference between the two piezometers. The result is a constant value

$$s_2 - s_1 = \frac{Q}{2\pi T} \ln\left(\frac{r_1}{r_2}\right) \tag{22}$$

which is identical to what Thiem predicted using the steady-state assumption (equation 6).

## Interpretation of a Pumping Test with the Theis Solution

The original method was based on the graphical superposition of the Theis type curve with the observed data on two log–log sheets of paper. Nowadays, many software will contain algorithms that apply the Theis method, but we believe that, here, it is useful to illustrate how the interpretation procedure can easily be implemented with any spreadsheet, graphical, or mathematical software. As a preliminary remark, note that equation (20) can be written as

$$s = a \log\left(\frac{t}{t_0}\right) \tag{23}$$

with

$$a = \frac{2.30Q}{4\pi T} \tag{24}$$

$$t_0 = \frac{r^2 S}{2.25T} \tag{25}$$

$a$ has the dimension of length [L], $t_0$ has the dimension of time [T]. A plot of the measured drawdown $s$ as function of the log of time will show a straight line with a slope $a$ for late time. $t_0$ will be the value of $t$ for which $s = 0$. We can therefore very easily read the values of $a$ and $t_0$ from the graph (Figure 5a). A simple interpretation procedure is then:

1. Plot the drawdown measured in the field and its logarithmic derivative as a function of time on the same semilog scale graph.
2. Estimate roughly on the graph the slope $a$ of the straight line, or read the value of the derivative when it stabilizes, it is $a/2.3$. In the example shown in Figure 5(a), we find a slope of about 1.75 m.
3. Read the time $t_0$ by extrapolating the straight line to the intercept with the horizontal axis, that is, where $s = 0$. In the example, we find $t_0 = 3.5\,10^2$ s.
4. Calculate with the spreadsheet or mathematical software the theoretical drawdown and derivative using the values of $a$ and $t_0$.

$$s = \frac{a}{2.3} E_1\left(\frac{0.5625t_0}{t}\right) \tag{26}$$

$$\frac{\partial s}{\partial \ln(t)} = \frac{a}{2.3} \exp\left(-\frac{0.5625t_0}{t}\right) \tag{27}$$

   If the exponential integral is not directly available you can use equations (16) and (18). Superpose the theoretical drawdown and derivative on the graph previously done.
5. Improve the fit iteratively by modifying the values of $a$ and $t_0$ and by visual inspection on your graph or by using a nonlinear least-square algorithm. It is possible to switch (by using the graphical options of the plotting software) from a semilog to a log–log plot if one wants to represent the final plot in log–log scale but this is not required. In our example, the final fit is shown in Figure 5(b).

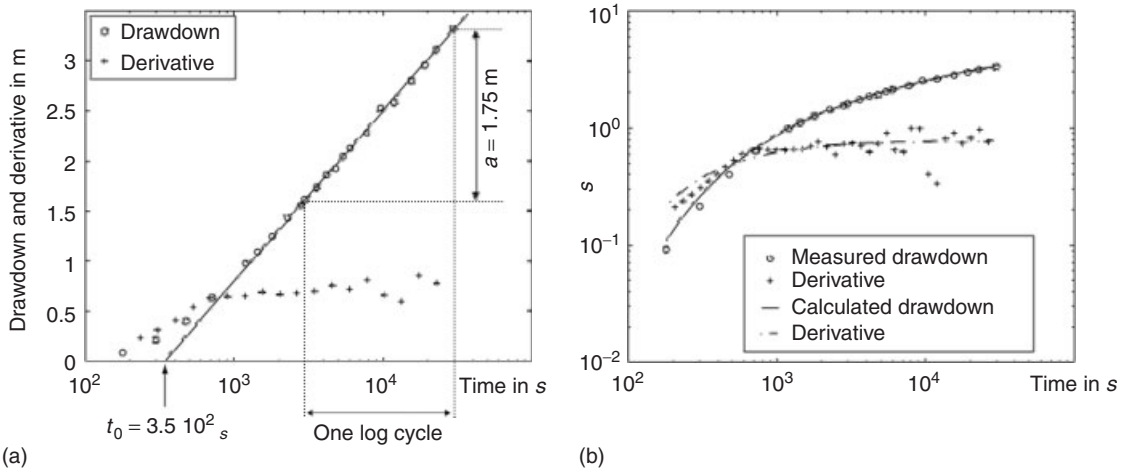


**Figure 5** Example of an interpretation of a data set with Theis method. (a) semilog plot of the drawdown and log derivative of a data set, identification of the constant a and $t_0$. (b) Superposition of the data with the model after automatic fitting

6. Should the fit be acceptable (both drawdown and derivative), the transmissivity $T$ and the storativity $S$ of the aquifer can be estimated with:

$$T = \frac{2.30Q}{4\pi a} = 0.183\frac{Q}{a} \tag{28}$$

$$S = \frac{2.25Tt_0}{r^2} \tag{29}$$

## NONIDEALITIES

### Heterogeneous Aquifers

What is the validity of the assumption of homogeneity? What is the meaning of the transmissivity obtained from a pumping test interpreted with Theis or Jacob solutions when the aquifer is heterogeneous? Meier *et al.* (1998) conducted a numerical study to investigate these questions. They simulated numerically the flow to a well in a series of heterogeneous aquifers. They considered that the transmissivity field is heterogeneous (Figure 6a) while the storativity is kept constant. They imposed a constant rate in the well and calculated the drawdowns in several piezometers (Figure 6b) using a finite element code. The numerical experiment is repeated for different types of transmissivity fields.

The main conclusion from this study is that the apparent transmissivity, estimated from the slope of the Jacob's straight line, of the transmissivity fields that they investigated is almost identical in all observation wells even if the heterogeneity in transmissivity is important. In these cases, the apparent transmissivity is very close to the uniform-flow effective transmissivity of the heterogeneous media (*see* **Chapter 154, Stochastic Modeling of Flow and Transport in Porous and Fractured Media, Volume 4**). However, the straight lines are shifted from one observation well to the next (Figure 6b), and therefore the estimated storativities vary within several orders of magnitude. The apparent heterogeneity in storativity is only a consequence of the heterogeneity in transmissivity. When interpreting a well test, such apparent heterogeneity in estimated storativity may be used as an indicator of the degree of heterogeneity of the transmissivity field. Furthermore, when many observation wells are available the geometric mean of the estimated storativity can be used as an estimator of the real storativity (Sánchez-Vila *et al.*, 1999). A consequence of the shift of the straight lines between observation wells due to heterogeneity, is that the Thiem method that only accounts for drawdown difference between two points will be strongly biased depending on the location of the points. This effect is illustrated by a laboratory experiment in a sand tank filled with a spatially variable pattern of different sands (Silliman and Caswell, 1998). They show that the application of the Thiem formula provides estimates of hydraulic conductivities that are extremely variable and that can be significantly lower (even negative) or higher than the local hydraulic conductivities.

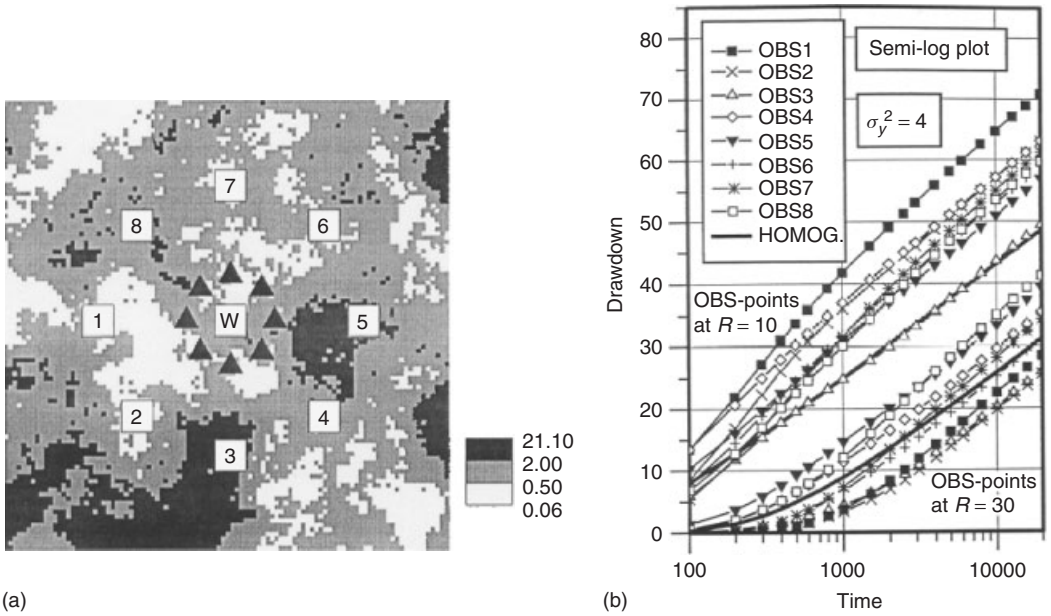


**Figure 6** Effect of heterogeneity. (a) Example of a simulated map of transmissivity for a multilognormal field. The W indicates the location of the pumping well. The triangles and the squares indicate the location of two series of observation wells. (b) Calculated drawdown in all the observation points. The line labeled HOMOG represents the calculated drawdown for the equivalent homogeneous medium (Reproduced from Meier *et al.,* 1998 by permission of American Geophysical Union)

In steady state, an interesting result is provided by Dagan (1982), who shows that the expected value of the hydraulic head in a heterogeneous aquifer follows the usual Dupuit solution (equation 5). Dagan also provides approximations for the variance of the head and shows how it is influenced by the heterogeneity of transmissivity and pumping rate.

### Partially Penetrating Wells

When the well does not fully penetrate the aquifer (Figure 7a), the flow field around the well has a vertical component. Hantush (1961) showed that in such a case the drawdown tends toward the classical Theis solution when

- the piezometer is located at a distance which is larger than one and a half times the thickness of the aquifer;
- or the observation well is screened over the complete thickness of the aquifer.

When the piezometer is close to the pumping well, the drawdown is affected by the partial penetration depending on the respective location of the well screen and the piezometer (Figure 7b). The late time asymptote is a Jacob straight line whose slope is the same as for a fully penetrating well. A common mistake is to use the screened interval thickness to obtain the hydraulic conductivity, while the real thickness of the aquifer should be used (if it is known).

### Bounded Aquifers

When the aquifer is not infinite, the drawdown is affected by the presence of boundaries. There are two typical cases: the presence of a river recharging the aquifer (constant head boundary) and the presence of an impervious geological boundary (no flow boundary).

If we assume that all the other assumptions from Theis are still valid, then the solution to these two problems is obtained by the application of the superposition principle and the theory of images. The concept is that the boundary is mathematically equivalent to the presence of an imaginary well located on the opposite side of the boundary. For the case of a no flow boundary, the image well is a pumping well, while for the case of a constant head boundary, the image well is an injection well (Figure 8).

Using this theory, the solution for both cases is

$$s = \frac{Q}{4\pi T} E_1\left(\frac{r^2 S}{tT}\right) + \beta \frac{Q}{4\pi T} E_1\left(\frac{r_i^2 S}{tT}\right) \qquad (30)$$

with $r_i$ being the distance between the observation well and the imaginary well, $\beta = 1$ for a no-flow boundary and $\beta = -1$ for a constant head boundary.

For the case of a no-flow boundary, the behavior of the drawdown is illustrated in Figure 3(c). It is characterized by a doubling of the late time slope. Two segments of straight line in semilog scale can be seen. The first one corresponds to the Jacob approximation before the drawdown is affected by the boundary. The second straight line corresponds to the superposition of the pumping well and the boundary. Figure 3(d) illustrates the constant head boundary case. The drawdown stabilizes because of recharge from a river; the derivative decreases continuously and follows a straight line on a log–log plot.

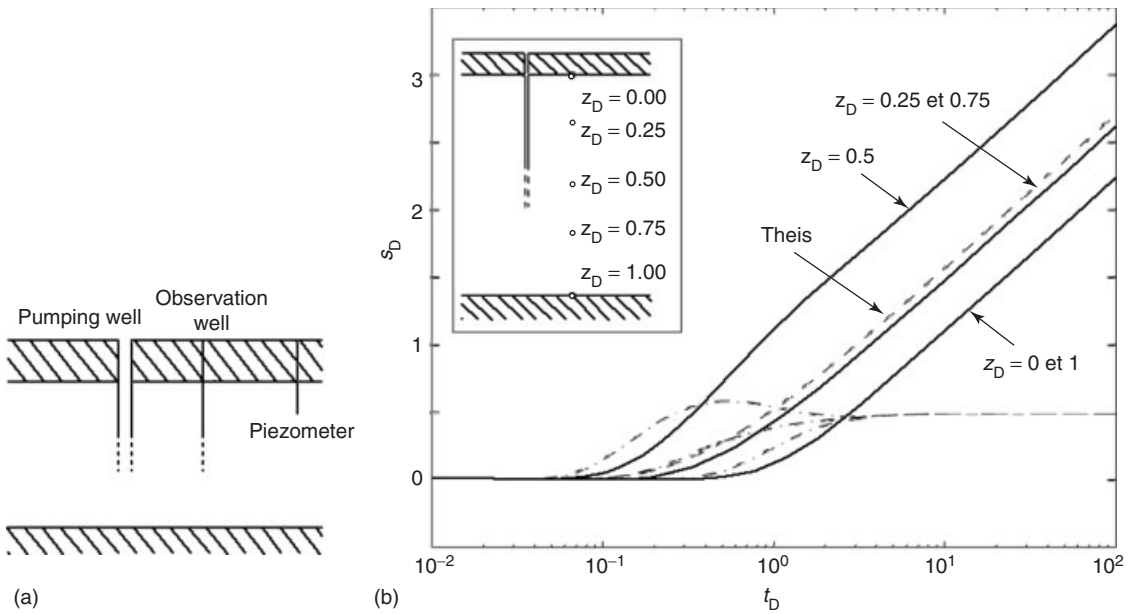


**Figure 7** Schematic section through a confined aquifer partially penetrated by a pumping well. (b) Type curves of Hantush's solution for partial penetration in semilog scale for the geometrical configuration illustrated in the figure

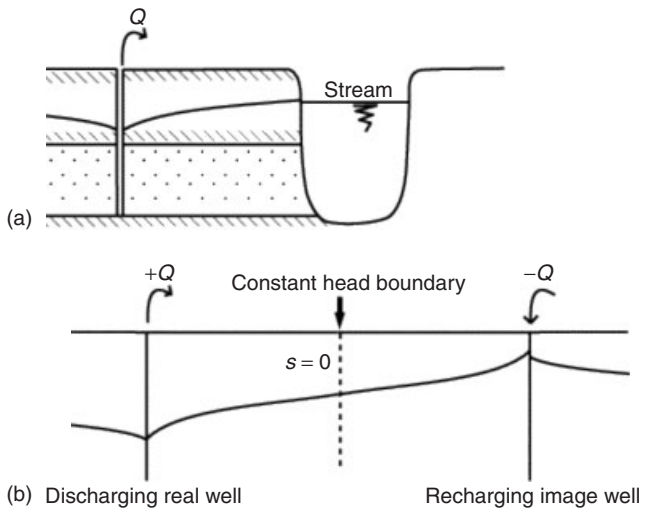


**Figure 8** Schematical representation of a confined aquifer bounded by a constant head boundary

Equation (30) implicitly assumes that the constant head is imposed throughout the whole thickness of the aquifer (Figure 8). A recent model considers a more realistic setup that accounts for the geometry of the riverbed (width compared to aquifer thickness) and an imperfect hydraulic connection between the river and the aquifer (Butler *et al.*, 2001). This model allows propagation of drawdown beneath a partially penetrating stream. The type curves of predicted drawdown range from the fully penetrating stream case (equation 30) to the Theis solution (equation 11) as a function of aquifer geometry and stream leakance: streambed hydraulic conductance multiplied by the square of the streamed width divided by the transmissivity of the aquifer below the stream.

Equation (30) can be extended for multiple boundaries. When the boundaries fully penetrate the aquifer, analytical solutions are obtained by the application of image theory. The analytical solution is then the sum of a series of drawdowns resulting from pumping and injection wells located according to the geometry of the boundaries. If one of these boundaries is a constant head boundary, the drawdown stabilizes to a constant value and a steady state is reached for late times. Closed expressions for these asymptotic values are useful, for example for the design of pumping schemes. For a single constant head boundary, the late time asymptote is

$$s = \frac{Q}{2\pi T} \ln\left(\frac{2L}{r_0}\right) \tag{31}$$

with $L$ being the distance between the well and the boundary and $r_0$ the radius of the well.

In the case of the closed rectangular system shown on Figure 9, the late time asymptote is obtained with the

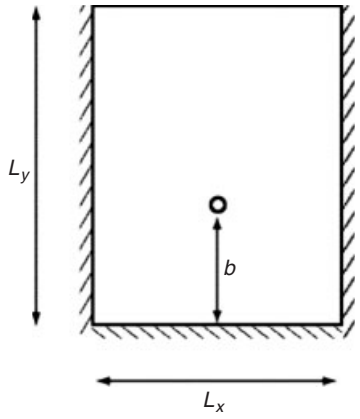


**Figure 9** Geometry of a simplified rectangular system with a pumping well, three no flow boundaries and one constant head boundary

Perrochet approximation

$$s = \frac{Q}{2\pi T} \ln\left(\frac{e^{2\pi\frac{L_x - b}{L_y}}}{2\pi}\frac{L_y}{r_0}\right), \frac{L_x}{L_y} > \frac{1}{2}, \frac{3L_x}{4} > b > \frac{L_x}{4} \tag{32}$$

with relative errors less than 1%.

When b = 0, the asymptote becomes

$$s = \frac{Q}{\pi T} \ln\left(\frac{e^{\pi\frac{L_x}{L_y}}}{2\pi}\frac{L_y}{r_0}\right) \tag{33}$$

## Variable Pumping Rate

As a starting point, suppose that the pumping rate is constant with a value $Q_1$ for $0 < t < t_1$ and then the pumping rate is suddenly increased to a value $Q_2$ at the time $t = t_1$. Assuming that all the other Theis assumptions are valid, the drawdown during the first phase of the test can be expressed with the Theis solution:

$$s = \frac{Q_1}{4\pi T} E_1\left(\frac{r^2 S}{4Tt}\right) t < t_1 \tag{34}$$

Because of the linearity of the groundwater flow equation for a confined aquifer, we can apply the principle of superposition in time and the drawdown in the second phase is simply the sum of the drawdown due to pumping $Q_1$ from $t = 0$ and the drawdown due to the pumping rate difference $Q_2 - Q_1$ starting at $t = t_1$.

$$s = \frac{Q_1}{4\pi T} E_1\left(\frac{r^2 S}{4Tt}\right) + \frac{Q_1 - Q_2}{4\pi T} E_1\left(\frac{r^2 S}{4T(t - t_1)}\right) t > t_1 \tag{35}$$

We can generalize this idea to a continuously varying pumping rate $Q(t)$:

$$s = \frac{Q(0)}{4\pi T} E_1\left(\frac{r^2 S}{4Tt}\right) + \frac{1}{4\pi T}\int_0^t \left.\frac{\partial Q}{\partial t}\right|_\tau E_1\left(\frac{r^2 S}{4T(t-\tau)}\right) \mathrm{d}\tau \qquad (36)$$

### Leakage Through the Confining Layer

Often aquifers are not fully confined, and receive a significant inflow from adjacent beds. Hantush and Jacob (1955) developed the first analytical solution for this situation. Their model considers a confined aquifer overlain by an aquitard and another aquifer (Figure 10). They assume that the pumped aquifer is recharged from the unpumped aquifer through the aquitard. The pumped aquifer is an ideal homogeneous isotropic and infinite two-dimensional aquifer. The flow is assumed to be vertical in the aquitard, there is no storage in the aquitard, the head remains constant in the unpumped aquifer, and the flow remains horizontal in the aquifer. The analytical solution to this problem contains a new dimensionless number related to the aquitard property:

$$\frac{r}{B} = r\sqrt{\frac{k'}{Te'}} \qquad (37)$$

with $e'$ the thickness of the aquitard and $k'$ its hydraulic conductivity. Figure 3(e) shows the typical behavior of the drawdown calculated with the Hantush and Jacob model. After following the Theis solution at early time, the drawdown stabilizes and the derivative drops very fast. If the aquitard is impermeable or very thick or if the observation point is very close to the pumping well, that is, $r/B$ is small, then the solution reaches a plateau at very late time. Conversely, if the aquitard is highly permeable or very thin, or if the observation well is located at a great distance from the pumping well, that is, $r/B$ is large, then the drawdown rapidly stabilizes to a constant value:

$$s_D = K_0\left(\frac{r}{B}\right) \qquad (38)$$

with $K_0$ the modified Bessel function of the second kind and of the zeroth order.

Later on, improved solutions accounting for storage in the aquitard, complex multilayer systems were developed (Hantush, 1960; Neuman and Witherspoon, 1972). These solutions provide the basic theory allowing indirect testing of low permeability formations.

### Unconfined Aquifer

Unconfined aquifers are commonly encountered in well-test analysis. However, radial flow to a well in such an aquifer is a complex physical and mathematical problem. The water table will decline during pumping and therefore the domain for which the equations have to be solved is not constant. Furthermore, the saturated zone is in direct hydraulic relation with the unsaturated zone (Figure 11) and finally, even if the aquifer is horizontal, there is a vertical component of the flow in the vicinity of the pumping well. A complete analytical solution for the saturated–unsaturated system was derived by Kroszynski and Dagan (1975). The main conclusion of their work is that, even if it is more exact to make a complete saturated–unsaturated analysis, the difference in the position of the calculated water table is small if we compare the prediction made by the complete model with the prediction made by a model that does not take into account the unsaturated zone.

The approach most often used is based on the concept of a delayed water-table response. It was initiated by Boulton (1954) and developed by Neuman (1972, 1974). The typical behavior of the drawdown is shown in Figure 3(b). There are three typical stages. In the early time, the drawdown follows a Theis type curve corresponding to the release of water from elastic storage. Then, there is a transition with a flattening of the curve and a hole in the derivative.

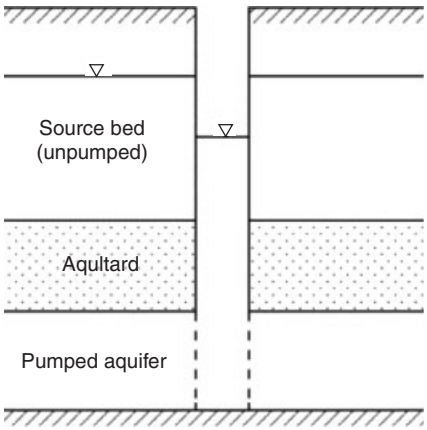


**Figure 10** Schematic of Hantush–Jacob model

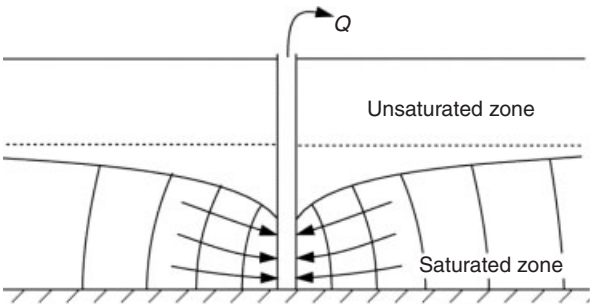


**Figure 11** Radial flow to a well in an unconfined aquifer

For late time, the drawdown follows a second Theis curve corresponding to the release of water from the drainage of the unsaturated zone. The derivative becomes a constant. One of the latest model developed for unconfined aquifers is an extension of the Boulton and Neuman models for a large diameter well and partially penetrating the aquifer (Moench, 1997, 1998).

## Well-bore Storage Effect

When the radius of the pumping well is large it contains a significant amount of fluid (Figure 12a). During early times, the aquifer's contribution to the total discharge is small (Figure 12b). Most of the water is pumped from the well itself. Later, the aquifer's contribution becomes dominant. Papadopulos and Cooper (1967) developed a model of this situation. Their model is identical to the Theis model for the governing equation, initial condition, and boundary condition at infinity. The difference is the boundary condition at the well that account for finite well radius and water storage in the well. This additional concept requires the definition of an additional dimensionless parameter, the well-bore storage coefficient:

$$C_{\mathrm{D}} = \frac{r_c^2}{2r_{\mathrm{W}}^2 S} \tag{39}$$

with $r_c$ being the radius of the casing and $r_{\mathrm{W}}$ the radius of the well screen. Figure 3(f) shows a typical behavior of the drawdown in the pumping well. The main characteristic of this type curve is that for early times, the asymptote is a straight line with unit slope in the log–log plot:

$$s_{\mathrm{w}} = \frac{Q}{\pi r_c^2} t \tag{40}$$

The logarithmic derivative follows the same straight line of unit slope. During this period, when the drawdown and derivative follow the same line, the well-bore storage effect is dominant. This is followed by a transition where the derivative departs from the straight line and makes a hump. For late times, the derivative stabilizes and the behavior is dominated by the aquifer contribution. The drawdown tends toward the Jacob's solution. Note that later on, boundary effects can affect the solution. For example Figure 3(j) shows the same type of behavior with an additional constant head boundary that stabilizes the drawdown for the late time and shows a drop of the derivative.

## Skin Effect

The drawdown in the pumping well can be strongly affected by the skin effect, that is, the existence of a zone of lower hydraulic conductivity than the aquifer in the immediate vicinity of the well (Figure 13). This zone of low hydraulic conductivity may be due to poor well development, deposition of particles or development of bacterial films. Also, increased hydraulic conductivity in the immediate vicinity of the well is possible and is accounted for in the theory but have less impact on the drawdowns in the well.

The concept of skin effect was introduced by van Everdingen (1953). Later, Agarwal *et al.* (1970) developed a solution including both well-bore storage and skin effect. To quantify the skin effect and assuming steady state, it is simple to show that the additional drawdown $s_{\mathrm{D}}$ in the well due to a cylinder of radius $r_s$ and having a transmissivity $T_s$ is

$$s_{\mathrm{D}} = \frac{Q}{2\pi T}\sigma \tag{41}$$

with $\sigma$ being the skin factor:

$$\sigma = \left(\frac{T - T_S}{T}\right) \ln\left(\frac{r_s}{r_{\mathrm{w}}}\right) \tag{42}$$

Note that $\sigma$ is positive if the well is clogged ($T_s < T$) and negative for the opposite case. The early time

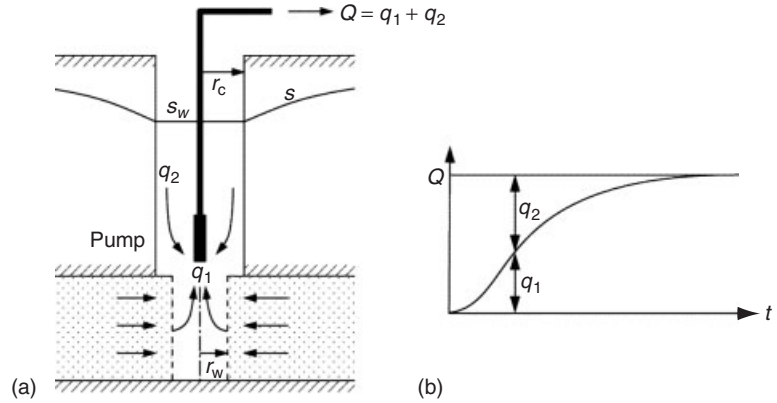


**Figure 12** Schematic of the well-bore storage effect

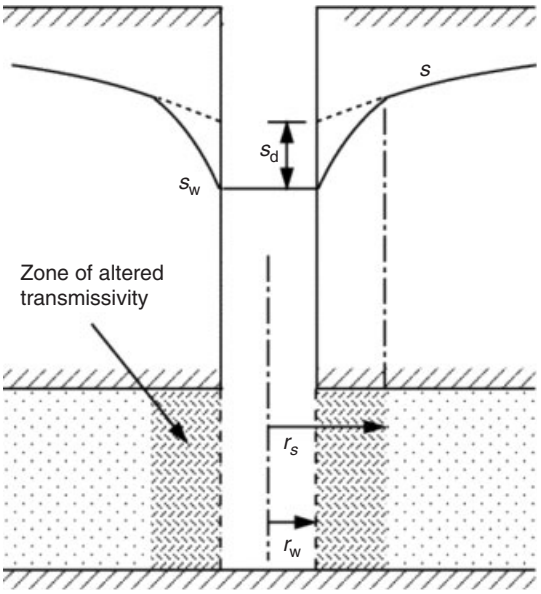


**Figure 13** Finite thickness skin model

behavior of the solution of Agarwal *et al.* is identical to the Papadopulos–Cooper solution (1967). The late time asymptote is a straight line (on semilog plot) parallel to Jacob's straight line but shifted by $\sigma$.

$$s_D = \tfrac{1}{2}[\ln(4t_D) - \gamma] + \sigma \tag{43}$$

As with the Theis model, the late time data allows unique identification of the transmissivity of the aquifer from the slope of the straight line, or from the value of the logarithmic derivative. However, the position of the line is both a function of storativity and of the skin effect. It is therefore impossible to determine both the storativity and the skin effect with a single well test.

An other important feature of the Agarwal solution is that the shape of the type curves are identical for all type curves having the same value of the product $C_D e^{2\sigma}$ when $\sigma > 0$, and $C_D e^{2\sigma} > 10^3$. Furthermore the shape of these type curves (see Figure 3f) is identical to the original Papadopulos–Cooper type curves only accounting for well-bore storage effects. In practice, this means that the effect of well-bore storage and skin effect are not distinguishable.

## Quadratic Head Losses

In the model of Agarwal *et al.* the drawdown in the pumped well increases linearly with $Q$. However, based on field observations, Jacob (1947) indicates that the drawdown in a pumping well generally increases as a function of the square of the flow rate (Figure 14a).

$$s = AQ + BQ^2 \tag{44}$$

This additional head loss can strongly affect the drawdown in the borehole and therefore its efficiency. The additional drawdown is attributed to inertial or turbulent flow occurring in the zone just outside the well, through the well screen and in the casing (Rorabaugh, 1953). This additional drawdown is commonly referred to as the quadratic head losses or the nonlinear head losses in the well. The *nonlinear head-loss coefficient* $B$ allows quantifying the importance of this effect. In petroleum engineering, this phenomenon is mainly described for gas well testing and is modeled with a rate dependent skin effect. In practice, to evaluate the importance of these head losses, a step-drawdown test is conducted. At first, the well is pumped at a given flow rate for a given amount of time (Figure 14b); subsequently the flow rate is modified and applied for another given duration; then again the flow rate is changed and and so on. Usually the minimum number of steps is three, allowing to identify the nonlinear head-loss coefficient and to check the adequacy of equation (44). The interpretation of such step-drawdown tests relies on the late time asymptote and on the superposition principle (Eden and Hazel, 1973; Hantush, 1964). Some attempts have been made to include the inertial term in a transient solution

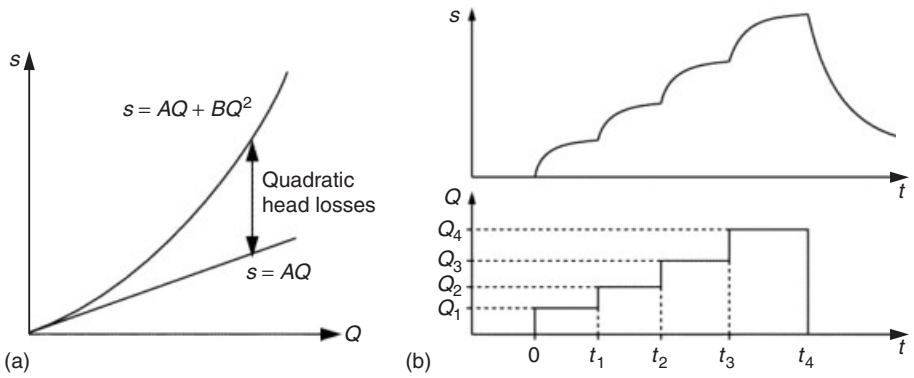


**Figure 14** (a) Drawdown in the well as a function of the discharge rate. (b) A step-drawdown test

(Chachadi and Mishra, 1992), but the analytical approach is not yet fully convincing as it does not respect the continuity of heads throughout the well screen. The most promising approach used to date is numerical. It includes the inertial term within the aquifer and has been applied to a deep fractured aquifer (Kohl *et al.*, 1997).

## The Double Porosity Model

In 1960, Barenblatt and his coworkers introduced a revolutionary concept:

> "Unlike in classical fluid flow theory, for each point in space, not one hydraulic head but two, $h$ and $h'$, are introduced. The head $h$ represents the average head in the fractures in the neighborhood of the given point, whereas [...] $h'$ is the average head in the matrix in the neighborhood of the given point" (Barenblatt *et al.*, 1960). This concept forms the foundation of the double porosity approach. In their article, Barenblatt *et al.* assumed that the storativity of the fractures was negligible. Warren and Root (1963) introduced a storativity for the fractures and developed a model, which is still used today.

The formulation of the double porosity models (see Figure 15) is based on two coupled standard groundwater flow equations (one for the fracture, one for the matrix) with an exchange term. The hydraulic conductivity and the specific storage coefficient are defined separately for each media. To simplify the system of equations, Warren and Root assume that the water moves from matrix blocks to fractures, but not from matrix block to matrix block. It is furthermore assumed that the flow rate between the matrix and the fractures is proportional to the hydraulic conductivity of the matrix, to the hydraulic head differences between the two systems, and to a geometrical factor depending on the size and the shape of the matrix blocks. This is the so-called pseudosteady state assumption of Warren and Root.

A typical drawdown curve is shown in Figure 3(b). It has a sigmoidal shape. During early time, the water is pumped from storage in the fractured system, the matrix does not affect the flow. In the intermediate times, water is released from the matrix while the drawdown in the matrix is small compared to drawdown in the fractures. During the late time, the drawdown in the matrix approaches the drawdown in the fractures and the aquifer behaves like a single porosity aquifer with the combined property of the matrix and the fractures. The log derivative shows a typical depression before it stabilizes to the constant value indicating that the drawdown reached the late time Jacob's straight line.

More recently, the model of Warren and Root has been extended to account for well-bore storage and skin effect (Bourdet and Gringarten, 1980). Another modification of the model is to account for transient flow within the matrix to the fractures (Boulton and Streltsova, 1977). In this model, the head distribution is solved within the blocks and therefore it is necessary to assume a given shape for the blocks. Boulton and Streltsova consider a representation of the fractured medium as alternating layers of matrix rocks and fractures. Once again, the resulting type curves show the typical sigmoidal shape and depression in the logarithmic derivative.

## General Radial-Flow Model

The General Radial-Flow (GRF) model (Barker, 1988) is a generalization of radial-flow equations to any flow dimension $n$ that includes the specific cases of linear flow ($n = 1$), usual cylindrical flow ($n = 2$), and spherical flow ($n = 3$), it extends as well to noninteger-flow dimensions for intermediate cases (see Figure 16). The beauty of this model is that it provides a unique solution for a large range of possible behaviors with only one additional parameter (the flow dimension $n$). In subsequent publications, the GRF model was extended to include well-bore storage, skin effects, and double porosity (Hamm and Bideaux, 1996). The solution of the standard GRF model (without skin, well-bore storage and double porosity) with a constant pumping rate in an infinite medium is

$$s_D = \frac{r_D^{2-n}}{\Gamma\left(\frac{n}{2}\right)} \Gamma\left(\frac{n}{2} - 1, \frac{t_D}{4r_D^2}\right) \tag{45}$$

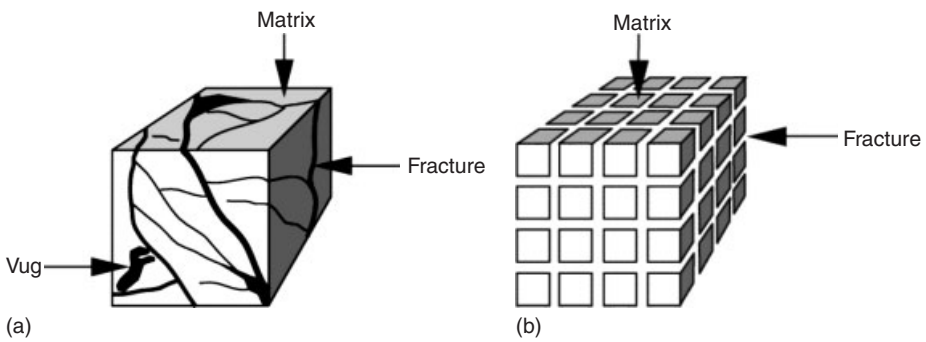


**Figure 15** A fractured block illustrating the double porosity concept (Adapted from Cinco-Ley, 1996)

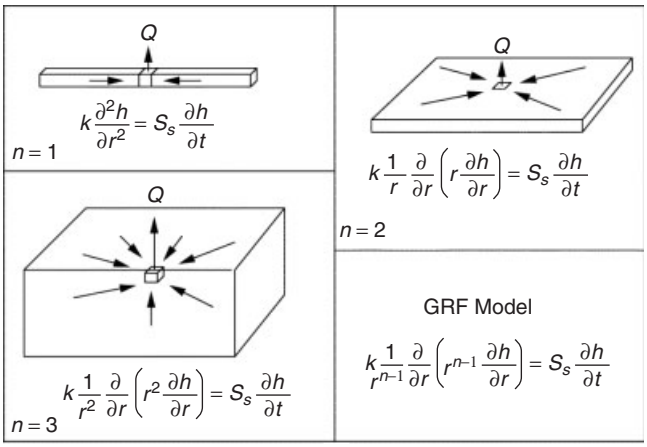


**Figure 16** Concept of radial flow in 1, 2, 3, and generalization to $n$ dimensions

with $n$ being the flow dimension, $\Gamma(x)$ the gamma function, and $\Gamma(a, x)$ the incomplete gamma function. Figure 3(h) and Figure 3(i) show two examples of drawdown for $n < 2$ and $n > 2$ respectively. A typical characteristic of the GRF model is that the log derivative of the drawdown follows a straight line with a slope of $1 - n/2$ in the diagnostic plot. When $n = 2$, the GRF model converges toward the Theis solution, and the log derivative becomes constant for late time (0 slope). Barker suggests that the fractional-flow dimension may be related to the observed fractal properties of fracture networks. However, the diffusivity of the GRF model remains equal to $k/S_s$ even when the flow dimension is fractional. An alternative analytical model based on a fractal network of fractures has been proposed by Chang and Yortsos (1990). Both models have been compared with numerical simulations in fracture networks. Acuna and Yortsos (1995) show that the model of Chang and Yortsos agrees with drawdowns simulated on artificially generated fractal networks (e.g., Sierpinski carpets). More recently, Jourde *et al.* (2002) show that fractional-flow dimension may even appear on a Euclidian network by using a network of pipes simulating a network of pseudorandom orthogonal fractures.

### Individual Fractures

A more specific situation is the case of an individual fracture intersected by the well and acting as a drain in a larger porous aquifer. Several models have been developed for this type of configuration (Gringarten, 1982). The case of the drawdown in a well intersecting a vertical fracture of infinite conductivity and finite length is illustrated in Figure 3(g) (Gringarten *et al.*, 1974). A 0.5 slope for the drawdown and the derivative characterizes this solution at early time on a log–log plot.

## OTHER HYDRAULIC PERTURBATIONS

### Recovery Test

Head recovery after a pumping test can be modeled using the superposition principle. When the aquifer is confined, from a mathematical point of view, the end of pumping is equivalent to continuing pumping and simultaneously injecting the same amount. This implies that the drawdown can be calculated by adding drawdown due to pumping plus drawdown due to a simultaneous injection at the same location. In the case of the Theis assumptions, the solution for the recovery is therefore

$$s_{\mathrm{D}} = \frac{1}{2}E_1\left(\frac{r_{\mathrm{D}}^2}{4(t_{\mathrm{P}} + t_{\mathrm{R}})}\right) - \frac{1}{2}E_1\left(\frac{r_{\mathrm{D}}^2}{4t_{\mathrm{R}}}\right) \qquad (46)$$

where $t_{\mathrm{R}}$ is the dimensionless time since the recovery started and $t_{\mathrm{P}}$ is the dimensionless production time. Equation (46) is exact and can be used to analyze a data set and to estimate both $T$ and $S$. An asymptotic solution is however often used. When both exponential integrals, in equation (46), can be approximated by a logarithmic function, one finds the late time asymptote:

$$s_{\mathrm{D}} = \frac{1}{2}\ln\left(\frac{t_{\mathrm{R}} + t_{\mathrm{P}}}{t_{\mathrm{R}}}\right) \quad \text{or} \quad s = \frac{2.30Q}{4\pi T}\log\left(\frac{t_{\mathrm{r}} + t_{\mathrm{p}}}{t_{\mathrm{r}}}\right) \qquad (47)$$

with $t_{\mathrm{r}}$ being the time since the beginning of the recovery and $t_{\mathrm{p}}$ the production time. This approximation allows rapid interpretation of late time recovery by constructing a semilog plot of the drawdown versus the log of the ratio $(t_{\mathrm{r}} + t_{\mathrm{p}})/t_{\mathrm{r}}$, denoted as the Horner time in the oil industry. Although, the slope is then proportional to the transmissivity, the storativity cannot be estimated. Another alternative to interpret recovery data has been proposed by Agarwal (1980). He found that if the recovery time is replaced by a corrected time $t_a$:

$$t_a = \frac{t_{\mathrm{p}}t_{\mathrm{r}}}{t_{\mathrm{p}} + t_{\mathrm{r}}} \qquad (48)$$

The interpretation is thus greatly facilitated. One can apply the standard interpretation models above described for constant rate pumping tests, including the log derivative for model identification. Note, however, that the approach is not valid for bounded aquifers.

### Constant Head Test

In some situations, the artificial perturbation imposed in the well is not a constant discharge or recharge rate but a constant head. Under these circumstances, the aquifer responds by a groundwater discharge at a variable rate into the well, and a variation of head within the aquifer.

Both perturbations can be modeled. Considering an ideal confined aquifer, the standard analytical solution for the discharging rate in the well is the solution of Jacob and Lohman (1952). Mishra and Guyonnet (1992) indicate that using the drawdown normalized by the discharge rate allows field data to be interpreted with the usual Theis model. The discharge rate in the well can be evaluated with excellent accuracy using the Perrochet approximation:

$$q_D = \frac{q}{2\pi T s_0} = \frac{1}{\ln(1 + \sqrt{\pi t_D})} \tag{49}$$

with $s_0$ being the imposed drawdown at the well and with relative error less than 1% over the range $10^{-4} < t_D < 10^{12}$.

Additional solutions for the constant head case accounting for boundaries and transient effects are available in Murdoch and Franco (1994).

Constant head situations are naturally encountered in artesian aquifers. Constant head tests offer a useful alternative to pumping tests since they minimize the effect of well-bore storage and therefore reduce the required duration of a test. Another advantage is that constant head tests can be carried out when the maximum admissible drawdown may be limited. This can be the case when the hydraulic conductivity is small.

### Slug Test

The slug test method (Hvorslev, 1951) was developed to rapidly estimate aquifer transmissivity. The principle involves instantaneously perturbing the water level in a well by an injection or an extraction of a known volume of water (Figure 17). After the perturbation, the water levels are recorded in the well or in a piezometer until they stabilize.

Depending on the geometry and type of aquifer, several analytical solutions can be used for slug-test data interpretation. Practical recommendations concerning the design and the performance of slug tests as well as a compendium of available analytical solutions is available in Butler (1998). Recent contributions include a detailed analysis of inertial effects, given the rapid and often oscillatory behavior of the head in the borehole itself (McElwee and Zenner, 1998; Zurbuchen *et al.*, 2002). From a general point of view, slug tests are very interesting because they take much less time to carry out than pumping tests or constant head tests and require less equipment. Consequently, they are cheaper to conduct. One can therefore perform a large number of slug tests in an aquifer in order to characterize the spatial distribution of hydraulic conductivities (see e.g. Mas-Pla *et al.*, 1997). Slug tests also allow testing low permeability formations that may not be tested within a reasonable period of time using pumping test techniques. The main disadvantage of slug tests is that the radius of investigation is much smaller than for a pumping test. As a consequence, they are much more strongly influenced by skin effects or local heterogeneities around the well (Butler and Healey, 1998). Another drawback of this technique is that it is difficult to estimate the storativity coefficient with sufficient certainty.

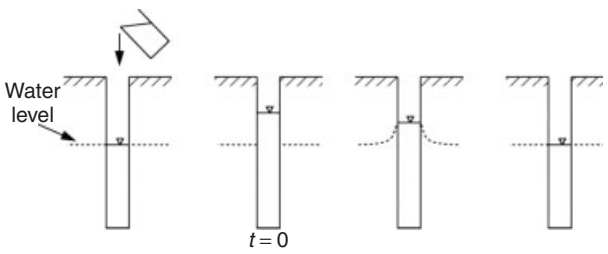


**Figure 17** Slug-test procedure

## REFERENCES

Abramowitz M. and Stegun I.A. (1970) *Handbook of Mathematical Functions*, National Bureau of Standards: Washington.

Acuna J.A. and Yortsos Y.C. (1995) Application of fractal geometry to the study of networks of fractures and their pressure transient. *Water Resources Research*, **31**, 527–540.

Agarwal R.G. (1980) A new method to account for producing time effects when drawdown type curves are used to analyze pressure buildup and other test data. Paper presented at the *55th Annual Fall Technical Conference and Exhibition of the Society of Petroleum Engineers of AIME*, Dallas.

Agarwal R.G., Al-Hussainy R. and Ramey H.J.J. (1970) An investigation of wellbore storage and skin effect in unsteady liquid flow. *SPE Journal*, **10**, 279–290.

Barenblatt G.I., Zheltov I.P. and Kochina I.N. (1960) Basic concepts in the theory of seepage of homogeneous liquids in fissured rocks (strata). *Journal of Applied Mathematics and Mechanics*, **24**, 1286–1303.

Barker J.A. (1988) A Generalized radial flow model fro hydraulic tests in fractured rock. *Water Resources Research*, **24**, 1796–1804.

Batu V. (1998) *Aquifer Hydraulics: A Comprehensive Guide to Hydrogeologic Data Analysis*, John Wiley & Son.

Beckie R. (2001) A comparison of methods to determine measurement support volumes. *Water Resources Research*, **37**, 925–936.

Boulton N.S. (1954) Unsteady radial flow to a pumped well allowing for delayed yield from storage. *AIHS Publications*, **37**, 472–477.

Boulton N.S. and Streltsova T.D. (1977) Unsteady flow to a pumped well in a fissured water-bearing formation. *Journal of Hydrology*, **35**, 257–269.

Bourdet D. (2002) *Well Test Analysis*, Elsevier.

Bourdet D., Ayoub J.A. and Pirard Y.M. (1989) Use of pressure derivative in well-test interpretation. *SPE Formation Evaluation*, **4**(2), 293–302.

Bourdet D. and Gringarten A. (1980) Determination of fissured volume and block size in fractured reservoirs by type-curve analysis. Paper presented at the *55th Annual Technical Conference and Exhibition of the Society of Petroleum Engineers*, Dallas.

Bourdet D., Whittle T.M., Douglas A.A. and Pirard Y.M. (1983) A new set of type curves simplifies well test analysis. *Word Oil*, **196**, 95–106.

Butler J.J. (1998) *The Design, Performance, and Analysis of Slug Tests*, Lewis Publishers.

Butler J.J. and Healey J.M. (1998) Relationship between pumping-test and slug-test parameters: Scale effect or artifact? *Ground Water*, **36**, 305–313.

Butler J.J., Zlotnik V.A. and Tsou M.-S. (2001) Drawdown and stream depletion produced by pumping in the vicinity of a partially penetrating stream. *Ground Water*, **39**, 651–659.

Chachadi A.G. and Mishra G.C. (1992) Analysis of unsteady flow to a large well experiencing well loss. *Ground Water*, **30**, 369–375.

Chang J. and Yortsos Y.C. (1990) Pressure transient analysis of naturally fractured reservoirs. Paper presented at the *SPE Annual Fall Meeting, Society of Petroleum Engineering*, Washington.

Chow V.T. (1952) On the determination of transmissibility and storage coefficients from pumping test data. *Transactions of the American Geophysical Union*, **33**, 397–404.

Cinco-Ley H. (1996) Well-test analysis for naturally fractured reservoirs. *Journal of Petrolem Technology*, 51–54.

Cooper H.H.J. and Jacob C.E. (1946) A generalized graphical method for evaluating formation constants and summarizing well fiel history. *Transactions of the American Geophysical Union*, **27**, 526–534.

Dagan G. (1982) Stochastic modeling of groundwater flow by unconditional and conditional probabilities: 1. Conditional simulation and the direct problem. *Water Resources Research*, **18**, 813–833.

Dawson K.J. and Istok J.D. (1991) *Aquifer Testing*, Lewis Publishers.

Dougherty D.E. (1989) Computing well hydraulics solutions. *Ground Water*, **27**, 564–569.

Dupuit J. (1863) *Etude Théoriques et Pratiques Sur le Mouvement Des Eaux Dans Les Canaux Découverts et à Travers Les Terrains Perméables*, Dunot: Paris.

Earlougher R.C.J. (1977) *Advances in Well Test Analysis*, Society of Petroleum Engineers of AIME.

Eden R.N. and Hazel C.P. (1973) Computer and graphical analysis of variable discharge pumping test of wells. Paper presented at the *Institute of Engineers Australia, Civil Engineering Transactions*, Vol. 15, no. (1-2), pp 5–10.

Gringarten A. (1982) Flow-test evaluation of fractured reservoirs. *Geological Society of America*, **Special Paper 189**, 237–263.

Gringarten A., Ramey H.J.J. and Raghavan R. (1974) Unsteady-state pressure distributions created by a single infinite conductivity vertical fracture. *Society of Petroleum Engineers Journal*, **14**, 347.

Hamm S.-Y. and Bideaux P. (1996) Dual-porosity fractal models for transient flow analysis in fractured rocks. *Water Resources Research*, **32**, 2733–2745.

Hantush M.S. (1960) Modification of the theory of leaky aquifers. *Journal of Geophysical Research*, **65**, 3713–3725.

Hantush M.S. (1961) Aquifer tests on partially penetrating wells. *Proceedings of the American Society of Civil Engineers*, **87**, 171–195.

Hantush M.S. (1964) *Hydraulics of Wells*, Academic Press.

Hantush M.S. and Jacob C.E. (1955) Nonsteady radial flow in an infinite leaky aquifer. *Transactions of the American Geophysical Union*, **36**, 95–100.

Horne R. (1995) *Modern Well Test Analysis*, *Second Edition*, Petroway, Inc.: Palo Alto.

Hvorslev M.J. (1951) Time lag and soil permeability in ground water observations. *U.S. Army Corps of Engineers Waterway Experimentation Station Bulletin*, **36**, 1–50.

Jacob C.E. (1947) Drawdown test to determine effective radius of artesian well. *American Society of Civil Engineers, Transactions*, **112**, 1047–1064.

Jacob C.E. and Lohman S.W. (1952) Non steady flow to a well of constant drawdown in an extensive aquifer. *Transactions of the American Geophysical Union*, **33**, 559–569.

Jourde H., Pistre S., Perrochet P. and Drogue C. (2002) Origin of fractional flow dimension to a partially penetrating well in stratified fractured reservoirs. New results based on the study of synthetic fracture network. *Advances in Water Resources*, **25**, 371–387.

Kohl T., Evans K.F., Hopkirk R.J., Jung R. and Rybach L. (1997) Observation and simulation of non-Darcian flow transients in fractured rocks. *Water Resources Research*, **33**, 407–418.

Kroszynski U.I. and Dagan G. (1975) Well pumping in unconfined aquifers: The influence of the unsaturated zone. *Water Resources Research*, **11**, 479–490.

Kruseman G.P. and Ridder N.A.d (1992) *Analysis and Evaluation of Pumping Test Data*, Vol. 47, ILRI publication.

Lavenue M. and de Marsily G. (2001) Three-dimensional interference test interpretation in a fractured aquifer using the pilot point inverse method. *Water Resources Research*, **37**, 2659–2675.

Lebbe L.C. (1999) *Hydraulic Parameter Identification*, Springer Verlag.

Lee T.-C. (1999) *Applied Mathematics in Hydrogeology*, Lewis Publishers.

Mas-Pla J., Yeh T.-C.J., Williams T. and McCarthy J.F. (1997) Analyses of slug test and hydraulic conductivity variations in the near field of a two-well tracer experiment site. *Ground Water*, **35**, 492–501.

McElwee C.D. (1980) Theis parameter evaluation from pumping tests by sensitivity analysis. *Ground Water*, **18**, 56–60.

McElwee C.D. and Zenner M.A. (1998) A nonlinear model for analysis of slug-test data. *Water Resources Research*, **34**, 55–66.

Meier P.M., Carrera J. and Sánchez-Vila X. (1998) An evaluation of Jacob's method for the interpretation of pumping tests in heterogeneous porous media. *Water Resources Research*, **34**, 1011–1025.

Mishra S. and Guyonnet D. (1992) Analysis of observation-well response during constant-head testing. *Ground Water*, **30**, 523–528.

Moench A.F. (1997) Flow to a well of finite diameter in a homogeneous, anisotropic water table aquifer. *Water Resources Research*, **33**, 1397–1407.

Moench A.F. (1998) Correction to "Flow to a well of finite diameter in a homogeneous, anisotropic water table aquifer". *Water Resources Research*, **34**, 2431–2432.

Moench A.F. and Ogata A. (1984) Analysis of constant discharge wells by numerical inversion of Laplace transform. In *Ground-Water Hydraulics*, Vol. 9, Rosensheim J.S. and Bennets G.D. (Eds.), American Geophysical Union, pp. 146–170.

Murdoch L.C. and Franco J. (1994) The analysis of constant drawdown wells using instantaneous source functions. *Water Resources Research*, **30**, 117–124.

Neuman S.P. (1972) Theory of flow in unconfined aquifers considering delay response of the watertable. *Water Resources Research*, **8**, 1031–1045.

Neuman S.P. (1974) Effect of partial penetration on flow in unconfined aquifers considering delayed gravity response. *Water Resources Research*, **10**, 303–312.

Neuman S.P. and Witherspoon P.A. (1972) Field determination of the hydraulic properties of leaky multiple aquifer systems. *Water Resources Research*, **8**, 1284–1298.

Oliver D.S. (1993) The influence of nonuniform transmissivity and storativity on drawdown. *Water Resources Research*, **29**, 169–178.

Papadopulos I.S. and Cooper H.H.J. (1967) Drawdown in a well of large diameter. *Water Resources Research*, **3**, 241–244.

Pinder G.F. and Bredehoeft J.D. (1968) Application of digital computers for aquifer evaluation. *Water Resources Research*, **4**, 1069–1093.

Raghavan R. (1993) *Well Test Analysis*, Prentice Hall.

Rorabaugh M.I. (1953) Graphical and theoretical analysis of step-drawdown test of artesian well. *Proceedings of the American Society of Civil Engineers*, **362**, 23.

Rosa A.J. and Horne R.N. (1991) Automated well test analysis using robust (LAV) non linear parameter estimation. Paper presented at the *66th Annual Technical Conference and Exhibition of the Society of Petroleum Engineers*, Dallas.

Sánchez-Vila X., Meier P.M. and Carrera J. (1999) Pumping tests in heterogeneous aquifers: An analytical study of what can be obtained from their interpretation using Jacob's method. *Water Resources Research*, **35**, 943–952.

Silliman S.E. and Caswell S. (1998) Observations of measured hydraulic conductivity in two artificial, confined aquifers with boundaries. *Water Resources Research*, **34**, 2203–2213.

Streltsova T.D. (1988) *Well Testing in Heterogeneous Formation*, John Wiley & Sons.

Theis C.V. (1935) The relation between the lowering of the piezometric surface and the rate and duration of discharge of a well using groundwater storage. *Transactions of the American Geophysical Union*, **2**, 519–524.

Thiem G. (1906) *Hydrologische Methoden*, Gebhardt: Leipzig, p. 56.

van Everdingen A.F. (1953) The skin effect and its influence on the productive capacity of a well. *Transactions of AIME*, **198**, 171–176.

Van Poolen H.K. (1964) Radius-of-drainage and stabilization-time equation. *The Oil and Gas Journal*, **62**, 138–146.

Walton W.C. (1996) *Aquifer Test Analysis with Windows Software*, Lewis Publishers.

Warren J.E. and Root P.J. (1963) The behaviour of naturally fractured reservoirs. *Society of Petroleum Engineers Journal*, **3**, 245–255.

Zurbuchen B.R., Zlotnik V.A. and Butler J.J.J. (2002) Dynamic interpretation of slug tests in highly permeable aquifers. *Water Resources Research*, **38**. 10.1029/2001WR000354.